



## Degradation of theophylline in a UV<sub>254</sub>/PS system: Matrix effect and application to a factory effluent



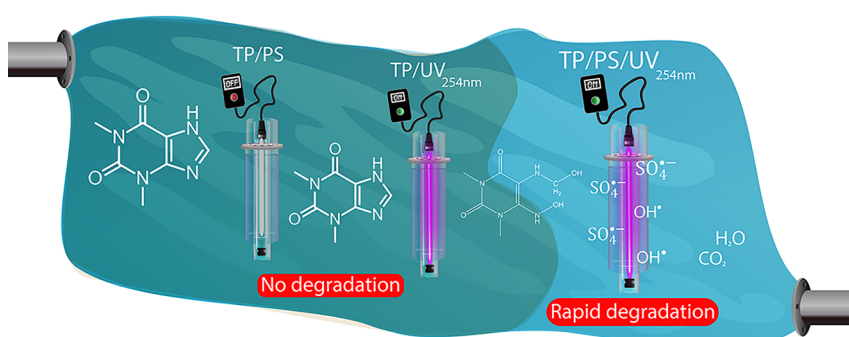
Suha Al Hakim, Saly Jaber, Nagham Zein Eddine, Abbas Baalbaki, Antoine Ghauch\*

American University of Beirut, Faculty of Arts and Sciences, Department of Chemistry, P.O. Box 11-0236 Riad El Solh, 1107-2020 Beirut, Lebanon

### HIGHLIGHTS

- UV<sub>254</sub>/PS system fully degraded Theophylline (TP) in an aqueous medium.
- Neutral pH was optimum for TP degradation.
- Chlorides and bicarbonates had low impact on TP degradation.
- UV<sub>254</sub>/PS system totally degraded TP in a concentrated pharmaceutical effluent.
- Pharmaceutical excipients showed slight effect on TP degradation process.

### GRAPHICAL ABSTRACT



### ARTICLE INFO

#### Keywords:

AOPs  
 Persulfate  
 Theophylline  
 UV-254 nm  
 Pharmaceutical effluent treatment

### ABSTRACT

Oxidative degradation of emerging waterborne contaminants, particularly pharmaceuticals, is currently an extensively studied field of research. In this study, a UV-254 nm activated persulfate (PS) system (UV<sub>254</sub>/PS) was used to eliminate Theophylline (TP) from simulated and real industrial effluents. Results showed that TP is strongly resistant to degradation through direct photolysis under UV-254 nm irradiation. UV<sub>254</sub>/PS system showed efficient degradation, in which [PS]<sub>0</sub> = 0.25 mM achieved total degradation of [TP]<sub>0</sub> = 10 mg L<sup>-1</sup> in a period of 20 min and followed a pseudo-first order reaction kinetics ( $k_{\text{obs}} = 0.173 (\pm 0.004) \text{ min}^{-1}$ ). Effect of several matrix parameters were tested to study the robustness of TP degradation in real-life cases such as pH, chlorides, bicarbonates, and dissolved oxygen, in which neutral pH gave the highest degradation rate ( $k_{\text{obs}} = 0.40 (\pm 0.03) \text{ min}^{-1}$ ), chlorides and bicarbonates showed minimal impact, and anoxic conditions inhibited TP degradation with a significant decrease in  $k_{\text{obs}}$  e.g.  $0.817 (\pm 0.41) \times 10^{-1} \text{ min}^{-1}$ . Additionally, TP was spiked into natural spring, sea and wastewater, where the three tested matrices showed a decrease in the degradation rate, with the latter being the most significant ( $k_{\text{obs}} = 6.9 (\pm 0.9) \times 10^{-3} \text{ min}^{-1}$ ). Radical scavenging experiments showed that sulfate radicals were the main contributors in TP degradation. Furthermore, wastewater effluent obtained from a local pharmaceutical manufacturing facility and containing [TP]<sub>0</sub> = 160 mg L<sup>-1</sup> was also tested and showed successful full degradation over 3 h in 25 mM PS-spiked medium with an average reaction stoichiometric efficiency of about 3.7% and at an estimated cost of 17.2 \$ m<sup>-3</sup>.

\* Corresponding author.

E-mail address: [antoine.ghauch@aub.edu.lb](mailto:antoine.ghauch@aub.edu.lb) (A. Ghauch).

<https://doi.org/10.1016/j.cej.2019.122478>

Received 31 March 2019; Received in revised form 8 August 2019; Accepted 9 August 2019

Available online 12 August 2019

1385-8947/ © 2019 Elsevier B.V. All rights reserved.

## 1. Introduction

Environmental contamination by pharmaceuticals and personal care products (PPCPs) has raised a major concern among the scientific community over the last two decades [1,2]. This is mainly due to the advancements in analytical chemistry techniques which allowed scientists to discover the presence of PPCPs at previously undetectable concentrations in surface and ground water around the world [3]. One of the drugs largely consumed and disposed into the environment is Theophylline (TP), a xanthine used in the treatment of lung diseases such as asthma, shortness of breath and wheezing [4]. TP is similar in structure to caffeine and theobromine and found in a normal diet as in tea and cacao beans in trace amounts [5,6]. Routes of TP entry into the environment include the discharge of untreated wastewater effluents from pharmaceutical production plants and domestic wastewater; where the latter contains TP from urine excretion due to consumption of pharmaceuticals and natural compounds, as well as direct disposal of TP-containing drugs [7,8]. TP was detected in spring water in Lebanon, possibly due to the release of untreated municipal wastewater and industrial effluents [9]. The presence of TP in nature increases concern of bioaccumulation which could result in undesirable health effects to humans and various animals, where it has been found that TP is moderately toxic to mammals ( $LD_{50} > 200 \text{ mg kg}^{-1}$ ) [10,11]. It is estimated that over 80% of the global wastewater is released to the environment without any prior treatment [12]. This factor, in addition to the resistance of PPCPs to conventional wastewater treatment methods [13] raises a great concern regarding the safety of natural aquatic systems.

Advanced Oxidation Processes (AOPs) have shown efficiency in the treatment of organic compounds. During the past decade, several research groups studied the degradation of TP using different methods. For instance, TP degradation was studied using Pd@MIL-100(Fe), a metal organic framework, for visible light ( $\lambda \geq 420 \text{ nm}$ ) driven photodegradation [14]. Another study used UV and UV/H<sub>2</sub>O<sub>2</sub> systems to study the degradation of TP in a mixture of 30 PPCPs [15,16]. Additionally, a UV/TiO<sub>2</sub> system [17], as well as a ferrate system [18] were tested for TP degradation.

Persulfate (PS) technology is one of the recent technologies of AOPs. PS can be activated thermally, chemically, by UV, or through a combination of activation techniques to generate highly reactive sulfate radicals (SO<sub>4</sub><sup>•-</sup>) species [19–22].

Of the activation methods, UV-activated PS has shown efficient degradation of several pharmaceuticals [21,23–25], but, to our knowledge, was not tested for TP degradation. Accordingly, a set of experiments were designed and applied to study the degradation of TP in simulated effluents and in a real highly charged industrial waste from a local pharmaceutical factory. Several parameters were assessed so as to optimize the degradation process yielding full TP degradation with an acceptable reaction stoichiometric efficiency (RSE) at an affordable cost.

## 2. Materials and methods

### 2.1. Chemicals

Theophylline (C<sub>7</sub>H<sub>8</sub>N<sub>4</sub>O<sub>2</sub> ≥ 99%), sodium persulfate (PS) (Na<sub>2</sub>S<sub>2</sub>O<sub>8</sub>, ≥99.0%), and phosphate buffer (monobasic and dibasic), all used in conducting the degradation experiments, were purchased from Sigma-Aldrich (China, France, and Germany, respectively). Potassium iodide (KI) (puriss, 99.0–100.5%, Switzerland), was used for the quantification of PS in solution. Methanol (CH<sub>4</sub>O) of HPLC grade (Germany) was used for the chromatographic elution process as mobile phase in combination with deionized water. Methanol and tertiary butyl alcohol (C<sub>4</sub>H<sub>10</sub>O) obtained from Sigma-Aldrich (Germany), were used in the quenching experiments. To assess the ionic additives effect, sodium chloride (NaCl) and sodium bicarbonate (NaHCO<sub>3</sub>) were purchased

from Fluka (Netherlands). Hydrogen Peroxide, used as an oxidant for a comparative study against PS, was obtained from Sigma Aldrich (Germany). Deionized water (DI) was used in the preparation of all solutions used in this work.

### 2.2. Chemical analyses

#### 2.2.1. TP quantification

To quantify TP, high performance liquid chromatography (HPLC, Agilent 1100 series) equipped with a quaternary pump, a vacuum degasser, an autosampler unit with cooling maintained at 4 °C, and a thermally controlled column compartment set at 30 °C was used. For TP separation from its byproducts and other organic additives, a Discovery® HS C-18 reverse phase column (5 μm; 4.6 mm internal diameter × 250 mm in length) connected to a security guard column HS C-18 (5 μm; 4.0 mm internal diameter 20 mm long) (Pennsylvania, USA) was used. The HPLC was equipped with two detectors placed in series, a diode-array detector (DAD) for the quantification of TP, and an ion-trap mass spectrometry detector (MSD) for the identification of TP's transformation products. The mobile phase consisted of water and methanol (70:30 ratio) kept under isocratic flowrate of 0.5 mL min<sup>-1</sup>. The injection volume was set at 80 μL. All samples were pre-filtered through a 0.45 μm PTFE 13 mm disc filters (Jaytee Biosciences Ltd., UK). Theophylline retention time (R<sub>t</sub>) was observed at 12 min using the abovementioned conditions. TP calibration curve and LINESIT output giving all statistical parameters required to determine the uncertainty on all quantified TP in UV<sub>254</sub>/PS treated samples are summarized in Fig. 1S.

#### 2.2.2. PS quantification

To quantify PS, an in-house validated analytical method developed by Baalbaki et al. [26] was used. The method relied on modifying the configuration of an HPLC unit allowing the formation of I<sub>3</sub><sup>-</sup> complex which is detected by the DAD at a wavelength of 352 nm.

### 2.3. Experimental setup: UV reactors

A bench-scale setup was assembled using 6 low-pressure mercury lamps (LPHgLS) fitted in quartz inserts that are submerged in home-made borosilicate cylinders. These lamps are commercially available and used in principle for water disinfection. The reactors are placed in a water bath connected to a chiller to keep constant the reaction temperature. The reactor is the same as the one used by Amasha et al. [20,21] of our research group. A scheme of the reactor (Fig. 2S) along with its components' origins are further elaborated in text S2 of the supplementary material.

### 2.4. Experimental procedure

Stock solutions of TP and PS were prepared on a daily basis and mixed with the required volumes of DI and/or matrix solutions in the 400 mL borosilicate reactors. After which the quartz protected LPHgLS were immersed in the reactors. 2 mL samples were then withdrawn at specific time intervals using appropriate syringes and injected through 0.45 μm PTFE 13 mm disc filters into the HPLC vials for analysis. Preparation of the stock solutions, the order of addition of reactants and further details of the experimental procedure are presented in text S3 of the supplementary material.

## 3. Results and discussion

### 3.1. UV<sub>254</sub> exposure effect: PS-free solution vs PS-spiked solution

To test for the possibility of direct and indirect photolysis of TP by LPHgLS, [TP] was monitored under the effect of UV-light, with and without PS addition. Fig. 1 shows that UV-254 nm only had no

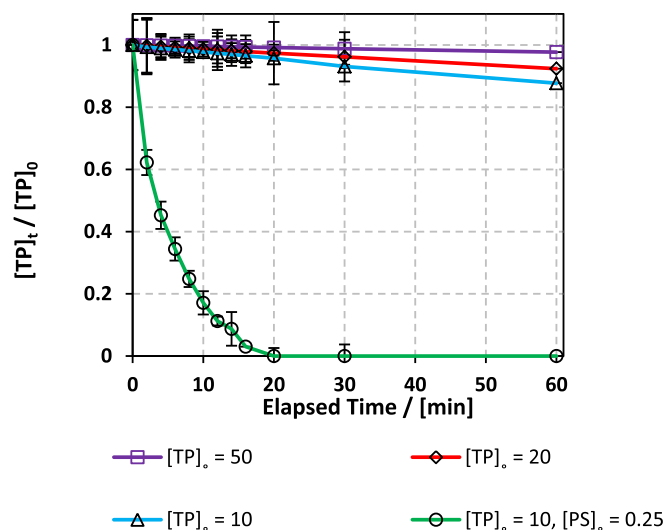


Fig. 1. Effect of UV fluence on TP degradation in PS-free and PS-spiked solutions. Control experiments (upper curves):  $[TP]_0 = 50, 20$  and  $10 \text{ mg L}^{-1}$  in PS-free solutions under UV 254 nm irradiation. The lowest curve represents the time course degradation of TP in PS spiked system under UV 254 nm irradiation ( $[TP]_0 = 10 \text{ mg L}^{-1}$  and  $[PS]_0 = 0.25 \text{ mM}$ ). Error bars are calculated as  $\frac{ts}{\sqrt{n}}$ , where absent bars fall within the symbols.

significant degradation effect on TP, where  $\frac{[TP]}{[TP]_0}$  after 60 min of exposure was higher than 88% for all  $[TP]_0$  tested. It can also be noticed that as  $[TP]_0$  increases, the % degradation under UV-254 nm alone decreases reaching, at 60 min of reaction time, 12, 8 and 2% for  $[TP]_0 = 10, 20$  and  $50 \text{ mg L}^{-1}$ , respectively. This decrease in the % degradation at higher  $[TP]_0$  can be attributed to the inner filter effect, where TP absorption spectrum (Fig. 1Sc) shows that absorption easily occurs at the wavelength emitted by the used LPHgLS mainly 254 nm. Inner filter effect is more prominent at higher  $[TP]_0$  where more absorbing molecules are present causing the solution to be less transmissible to UV-254 nm radiation and photon penetration. Inner filter effect was also noticed by Ao et al. (2017) during sulfamethoxazole photolysis [27]. Moreover, Fig. 1 shows that, in the presence of persulfate (0.25 mM) under UV-254 nm irradiation,  $[TP]$  ( $[TP]_0 = 10 \text{ mg L}^{-1}$ ) reached a level below the detection limit after only 20 min of reaction. Thus, even though TP absorbs at UV-254 nm, its direct photolysis is not significant, which necessitates the use of

oxidizing agents for effective degradation. The study of Pereira et al. (2007) showed that other pharmaceuticals such as naproxen and carbamazepine were resistant, or showed slight degradation, upon direct photolysis using only LPHgLS in oxidants-free solutions [28].

### 3.2. Kinetic study

The rate of degradation of TP was studied at four different  $[PS]_0$  (Fig. 2). Pseudo-first-order kinetics model showed good fittings for TP degradation, where  $R^2$  obtained for the plot of  $\ln \frac{[TP]}{[TP]_0}$  versus time (min) showed good linearity (Table S1). Thus Eq. (1) can be followed, with  $k_{obs}$  being the pseudo-first-order rate constant, and  $t$  representing time (min). The obtained data showed also that  $k_{obs}$  increased linearly with increasing  $[PS]_0$  (Fig. 2b), thus  $k_{obs}$  is found to be proportional to  $[PS]_0$  in the studied range. In fact, pseudo-first order is frequently considered for degradation reactions of organic compounds in PS-activated systems [25,29–31].

$$\ln \frac{[TP]}{[TP]_0} = -k_{obs}t \quad (1)$$

### 3.3. Choice of $[PS]_0$ for control experiment

The initial  $[TP]$  tested was  $10 \text{ mg L}^{-1}$ , which is in the expected range for wastewater effluent of a pharmaceutical production facility after dilution within the factory discharge. However, samples taken from a local plant revealed higher values of  $[TP]$  reaching  $160 \text{ mg L}^{-1}$  (Section 3.9); moreover, sustainable technical practices yielding less water consumption for cleaning reactors are rarely adopted and thus a more diluted effluent is expected. Accordingly,  $[PS]_0$  was varied experimentally to reach full TP degradation in a period of 20 min at 0.01, 0.1, 0.25 and 0.5 mM. As it can be noticed from Fig. 2, results showed that as  $[PS]_0$  increased the degradation rates increased, and thus the time needed for total TP degradation decreased. One can assume that higher density of  $SO_4^{\cdot-}$  is achieved with higher  $[PS]_0$  and that without significant radical-radical quenching reactions. For example, at  $[PS]_0 = 0.25$  and 0.5 mM, total TP degradation was reached within a range of 20 and 8 min, respectively (Fig. 2a). Accordingly,  $[PS]_0 = 0.25 \text{ mM}$  was chosen as an ideal oxidant concentration in order to conduct matrix effect experiments over an acceptable reaction time. In fact, this specific concentration showed rapid degradation of TP and is technically feasible in terms of sample withdrawal and tracking of  $[TP]$  as well as  $[PS]$  in solution for kinetics study.

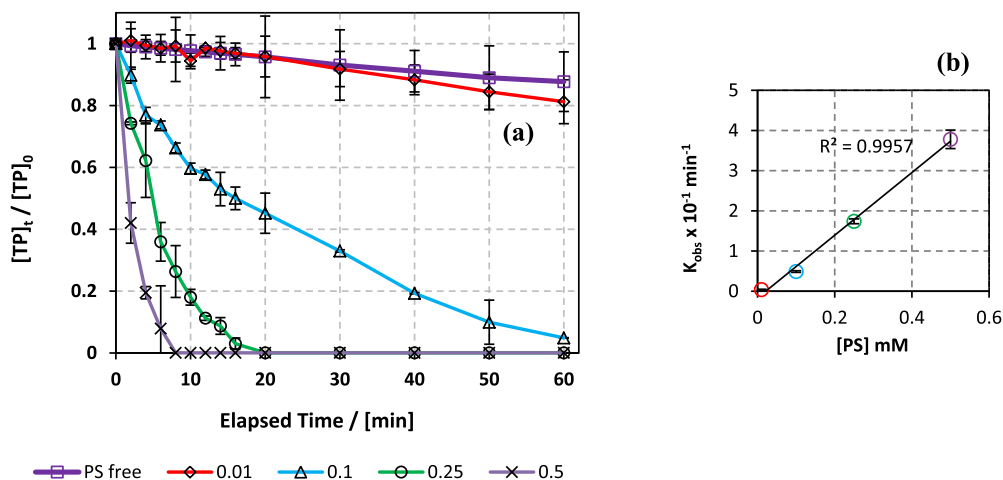


Fig. 2. Degradation of  $[TP]_0 = 10 \text{ mg L}^{-1}$  at  $[PS]_0 = 0.01\text{--}0.5 \text{ mM}$ . (a) Time course showing  $\frac{[TP]_t}{[TP]_0}$  variation in UV<sub>254</sub>/PS system. Error bars are calculated as  $\frac{ts}{\sqrt{n}}$ , where absent bars fall within the symbols. (b) A fitting of  $k_{obs}$  obtained for plots of  $\ln \frac{[TP]_t}{[TP]_0}$  versus time (min) for tested conditions upon first order fitting versus  $[PS]$  showing high correlation ( $R^2 = 0.9957$ ).

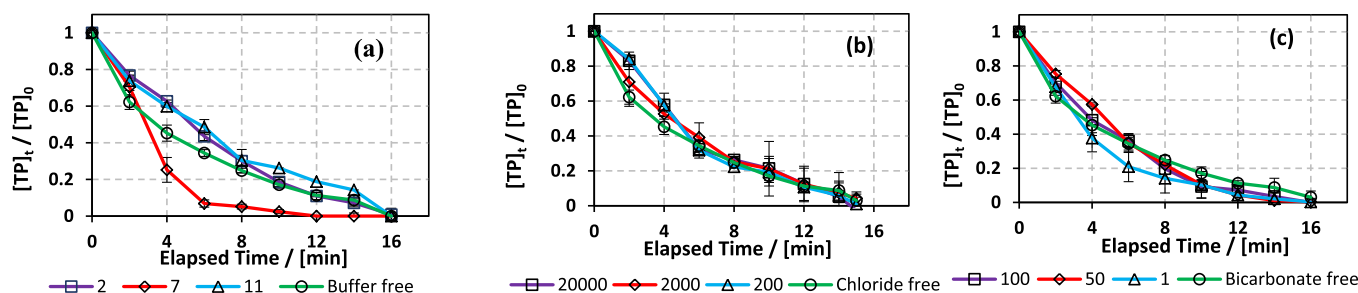


Fig. 3. Degradation of TP under effect of (a) pH, (b) salinity ( $[\text{NaCl}] = 0\text{--}20,000 \text{ mg L}^{-1}$ ), and (c) bicarbonates ( $0\text{--}100 \text{ mM}$ ). Experimental conditions:  $[\text{TP}]_0 = 10 \text{ mg L}^{-1}$ ,  $[\text{PS}]_0 = 0.25 \text{ mM}$ . Error bars are calculated as  $\frac{ds}{\sqrt{n}}$ , where absent bars fall within the symbols.

### 3.4. Additives and matrix effects

#### 3.4.1. pH effect

Several studies tested the pH effect on the degradation of various organic compounds and diverse results were obtained. It was found that frequently acidic pH conditions improved the degradation rate of the tested pollutants however, improved degradation was also observed at neutral and slightly basic pHs [32].

TP degradation was studied in non-buffered and in 10 mM buffered solutions of different pHs imitating extreme cases of acidic, basic as well as neutral conditions (Fig. 3a). For the case of non-buffered (DI) solution, an acidic pH is obtained upon PS addition ( $\text{pHi} = 5.4$ ). The acidification of the medium by PS is very well known and can be explained by Eqs. (2) and (3) [33].



The results obtained, for buffered solutions, showed that pH changes had significant impact on TP degradation. For example, neutral ( $\text{pH} = 7$ ) conditions gave the highest degradation rate constant ( $k_{\text{obs}} = 0.40 (\pm 0.03) \text{ min}^{-1}$ ) compared to buffer-free solutions ( $k_{\text{obs}} = 0.173 (\pm 0.004) \text{ min}^{-1}$ ), whereas acidic ( $\text{pH} = 2$ ) and basic ( $\text{pH} = 11$ ) pH conditions inhibited TP degradation to some extent with  $k_{\text{obs}} = 0.19 (\pm 0.01) \text{ min}^{-1}$  and  $0.139 (\pm 0.005) \text{ min}^{-1}$ , respectively (Table 1).  $k_{\text{obs}}$  were calculated using pseudo-first order model. Moreover, phosphate species of different concentrations (10 and 20 mM) used for buffering TP solutions showed slight effect on the degradation of TP as reported in Fig. 3S of the supporting information.

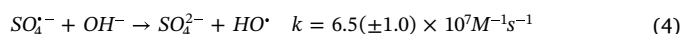
The decrease in the rate of the oxidation reaction at  $\text{pH} = 11$  compared to that at neutral pH could be attributed to the quenching effect of hydroxide ions ( $\text{OH}^-$ ) on  $\text{SO}_4^{\cdot-}$ ; in fact, at significant alkaline pH,  $\text{OH}^-$  reacts with  $\text{SO}_4^{\cdot-}$  and generates sulfate anion ( $\text{SO}_4^{2-}$ ) (Eq. (4)) [34]. The obtained  $\text{HO}^{\cdot}$  is of a shorter lifetime and lower selectivity

Table 1

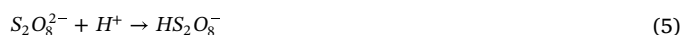
Values of pH and the observed degradation rate constants obtained for different matrix conditions. Experimental conditions:  $[\text{TP}]_0 = 10 \text{ mg L}^{-1}$  and  $[\text{PS}]_0 = 0.25 \text{ mM}$ .

Additive	Concentration	(unit)	pHi/pHf	$k_{\text{obs}} \times 10^{-1} (\text{min}^{-1})$	
Additive free	–	–	5.4/3.8	1.73 ( $\pm 0.04$ )	
Buffer	10	mM	2	1.9 ( $\pm 0.1$ )	
			7	4.0 ( $\pm 0.3$ )	
			11	1.39 ( $\pm 0.05$ )	
NaCl	20,000	$\text{mg L}^{-1}$	4.0/3.5	1.98 ( $\pm 0.01$ )	
			2000	4.1/3.6	1.79 ( $\pm 0.01$ )
			200	4.6/3.6	2.0 ( $\pm 0.1$ )
$\text{HCO}_3^-$	100	mM	8.7/8.4	2.4 ( $\pm 0.1$ )	
			50	8.5/8.2	3.0 ( $\pm 0.1$ )
			1	7.1/4.3	2.6 ( $\pm 0.1$ )
Methanol	100	mM	6.3/3.7	5.4 ( $\pm 0.3$ ) $\times 10^{-2}$	
			TBA	5.4/4.1	1.5 ( $\pm 0.1$ ) $\times 10^{-1}$

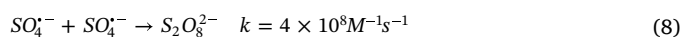
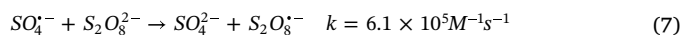
than that of  $\text{SO}_4^{\cdot-}$  which could be contributing to the decrease in the rate constant of TP degradation in a basic medium compared to that in an acidic medium [35]. To further investigate base activation of PS, the same conditions as for the already studied buffers were applied for TP solution at  $\text{pH} = 11$ , however, in the absence of UV. The results showed that no TP degradation was obtained. Thus, the base activation of PS was not prominent (Fig. 4S).



On the other hand at acidic pH, a rapid transformation of PS into  $\text{SO}_4^{\cdot-}$  is favored due to acid catalysis upon formation of  $\text{HS}_2\text{O}_8^-$  which improves TP degradation more than that at basic pH (Eqs. (5) and (6)) [36]. This observation corroborates the results obtained by Ghauch et al. [37] on the degradation of ibuprofen in thermally activated PS systems under acidic conditions.



However, the additional formation of  $\text{SO}_4^{\cdot-}$  generates a high concentration of radicals and cause quenching mechanism between  $\text{SO}_4^{\cdot-}$  (Eqs. (7) and (8)) [34,38]. Thus, the presence of TP in an acidic medium allows the PS-induced radicals in the medium to be partially quenched.



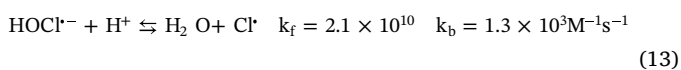
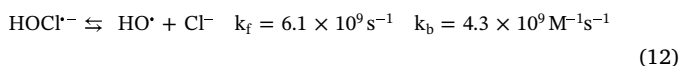
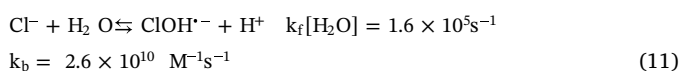
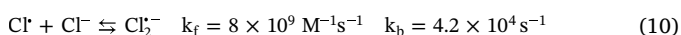
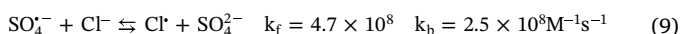
Additionally, the variance in TP degradation rate in water media of different pH values could be associated with its pka (8.81) [39]. At the tested acidic  $\text{pH} = 2$ , protonated TP ( $\text{TPH}^+$ ) is prevalent while at the basic  $\text{pH} = 11$ , non-protonated TP is the major species. However, at neutral  $\text{pH} = 7$  both species are present with  $\frac{[\text{TPH}^+]}{[\text{TP}]} \approx 10^{1.81}$ , based on the use of the Henderson equation. The presence of both species could result in two different degradation mechanisms simultaneously and thus better degradation kinetics [40]. Therefore, circumneutral pH showed the best pH range to consider for the studied degradation of TP, due to the presence of both  $\text{HO}^{\cdot}$  and  $\text{SO}_4^{\cdot-}$ , and the protonated and non-protonated forms of TP [41].

#### 3.4.2. Chloride effect

Pharmaceutical factory effluent might contain chlorides from different sources. Factories along the coast might domestically use brackish water that could be mixed with the pharmaceutical flushing water before exiting the factory. Additionally, detergents used to clean the factory's reactors as well as some pharmaceutical excipients used might contain chlorides. To test for the applicability of the studied oxidation method on water having different salinity levels (ionic strengths), experiments were conducted under four different matrix conditions simulating conditions of distilled, fresh, brackish and saline water having  $[\text{NaCl}]$  of about 0, 200, 2000 and 20000  $\text{mg L}^{-1}$ , respectively. These  $[\text{NaCl}]$  values were chosen based on Gorrell et al. and on EPA data [42,43]. As it can be noticed from Fig. 3b, the degradation

of TP was only slightly affected by NaCl presence. Table 1 showed that  $k_{\text{obs}}$  changed slightly from  $0.173 (\pm 0.004) \text{ min}^{-1}$  at  $[\text{NaCl}] = 0 \text{ mg L}^{-1}$  to  $0.198 (\pm 0.001) \text{ min}^{-1}$  at  $[\text{NaCl}] = 20,000 \text{ mg L}^{-1}$ . Hence, it is expected that PS in the presence of NaCl be partially consumed upon quenching by  $\text{Cl}^-$  to form chlorine radical ( $\text{Cl}_2^-$ ) (Eqs. 9–10). At the same time, one can predict that the remaining unquenched  $\text{SO}_4^-$  radicals along with the formed chlorine radicals were enough to degrade TP in solution at a similar rate close to that of TP degradation experiments carried out in NaCl-free solution.

A quick review on the effect of chlorides on the oxidation reaction in PS-based AOPs systems showed diverse results which varied between, enhancing, inhibiting, and negligible effect, where the effect of  $\text{Cl}^-$  on the degradation rate depends on its concentration, the probe, and the PS activation mechanism utilized (Table S2) [21,25,30,44–55]. Enhancement of the oxidative degradation reaction rate can be explained by the formation of  $\text{Cl}^\cdot$  having a redox potential ( $E^0 = 2.432 (\pm 0.018)$ ) close to that of  $\text{SO}_4^-$  ( $E^0 = 2.437 (\pm 0.019)$ ) [14], in addition to the formation of  $\text{HO}^\cdot$  (Eqs. (9), (11) and (12)) [56–58]. It is well known that  $\text{HO}^\cdot$  acts by  $\text{H}^\cdot$  abstraction, thus providing an enhancement in the oxidation rate for compounds susceptible to such degradation mechanism. Inhibition of the degradation process, however, can be explained mainly by the quenching of  $\text{SO}_4^-$  by  $\text{Cl}^-$  producing  $\text{Cl}^\cdot$  which in turn reacts to produce  $\text{Cl}_2^-$  of lower redox potential ( $E^0 = 2.126 (\pm 0.017)$ ) [14] than that of  $\text{SO}_4^-$  (Eqs. (9) and (10)) [56,57]. Additionally, the quenching of  $\text{HO}^\cdot$  by  $\text{Cl}^-$  is also expected, where  $\text{HO}^\cdot$  is more prevalent at basic pH [34,59]. For the case of negligible effect, as in current TP case,  $\text{Cl}^\cdot$  formed compensates for the lost effectivity of  $\text{SO}_4^-$  consumed (Eqs. (9)–(13)) [56–58].

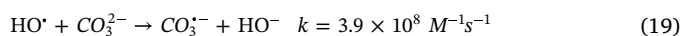
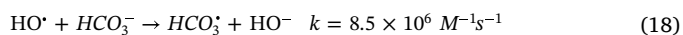
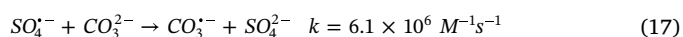
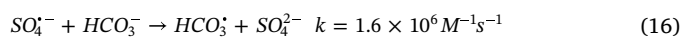
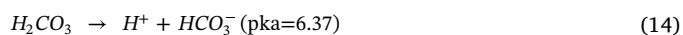


### 3.4.3. Bicarbonate effect

The effect of  $\text{NaHCO}_3$  on TP degradation was also studied at different concentrations: 1, 50 and 100 mM. Addition of  $\text{NaHCO}_3$  increased  $\text{pH}_i$  from 5.6 to a range between 7.1 and 8.7 depending on  $[\text{NaHCO}_3]$  in the medium.  $\text{HCO}_3^-$  added to the solution results in the formation of  $\text{H}_2\text{CO}_3$  and  $\text{CO}_3^{2-}$  (Eqs. (14) and (15)) [30]. As it can be noticed (Table 1, Fig. 3c),  $k_{\text{obs}}$  increased by 50% for the case of 1 mM ( $k_{\text{obs}} = 0.26 (\pm 0.01) \text{ min}^{-1}$ ) compared to the control case (bicarbonate-free solution;  $k_{\text{obs}} = 0.173 (\pm 0.004) \text{ min}^{-1}$ ). However, this trend is supported until greater concentration of bicarbonate (up to 50 mM) for which an increase of about 74% in  $k_{\text{obs}}$  is obtained ( $0.300 (\pm 0.001) \text{ min}^{-1}$ ). As for bicarbonate concentration close to 100 mM, one can notice a decrease in  $k_{\text{obs}}$  of about 20% compared to that of 50 mM (e.g.  $0.240 (\pm 0.001) \text{ min}^{-1}$  vs  $0.300 (\pm 0.001) \text{ min}^{-1}$ ). As a result, one can deduce that the improved efficiency of the oxidation reaction of TP is limited to a certain range of bicarbonate concentration mainly between 1.0 and 50 mM.

A mini-review on the effect of bicarbonate on the degradation of different probes in PS-based AOPs systems showed that  $\text{HCO}_3^-$  may have an enhancing or an inhibiting effect on the degradation of an organic probe (Table S3) [21,25,53,54,30,44,46–51]. Enhancement in the degradation rate of an organic contaminant is generally attributed to the working neutral/basic pH conditions that contribute to the increase in  $\text{HO}^\cdot$  upon reaction of  $\text{SO}_4^-$  with  $\text{HO}^-$  (Eq. (4)) which in its turn enhances the degradation rate of the probe [34].

In the case of TP, an increase in the pH of the solution is noticed with increasing  $[\text{NaHCO}_3]$ . Section 3.4.1 shows that neutral pH, obtained by using phosphate buffer solution, enhances the degradation reaction ( $k_{\text{obs}} = 0.40 (\pm 0.03) \text{ min}^{-1}$ ). However, for the case of neutral pH obtained by adding  $\text{HCO}_3^-$  (1 mM), lesser improvement in the degradation reaction rate constant ( $k_{\text{obs}}$  of  $0.26 (\pm 0.01) \text{ min}^{-1}$ ) is obtained. Thus, even though the neutral pH is favored, there is some inhibition caused by bicarbonate species present. This inhibition can be explained by an increase in the ionic strength of the solution yielding  $\text{SO}_4^-$  quenching mainly by  $\text{HCO}_3^-$  as well as  $\text{CO}_3^{2-}$  (Eqs. (16) and (17)), in addition to slower kinetics because of more difficult collision between reactive species in the medium [56]. Also, increasing  $[\text{HCO}_3^-]$  and  $[\text{CO}_3^{2-}]$  may react to quench  $\text{HO}^\cdot$ , when present in the medium (Eqs. (18) and (19)) [60,61]. The carbonate radical  $\text{CO}_3^{\cdot-}$  produced from quenching of  $\text{SO}_4^-$ , and possibly  $\text{HO}^\cdot$ , is of a lower redox potential ( $E^0 = 1.57 (\pm 0.03)$ ) [14], and thus is less potent to oxidize the organic probe. For instance, TP, as well as 17 $\beta$ -estradiol showed that an increase in  $[\text{NaHCO}_3]$  changed its effect on their degradation rate from enhancement to inhibition [44]. This is because the additional increase in the pH would cause the quenching of  $\text{SO}_4^-$  to outweigh the gain obtained by the formation of  $\text{HO}^\cdot$ . It is expected that probes more susceptible to  $\text{H}^\cdot$  abstraction have improved degradation, whereas probes that are mostly susceptible to electron transfer have inhibited degradation upon addition of  $\text{HCO}_3^-$ . In conclusion, the effect of addition of  $\text{HCO}_3^-$  is dependent on its concentration, the probe studied, and the pH change in the medium.



### 3.4.4. Effect of dissolved oxygen

Dissolved oxygen (DO) is a crucial parameter for optimizing degradation processes based on the use of AOPs. In order to address this parameter, similar experiments, as previously described, were performed however in the absence of DO. DO was removed by bubbling the TP solution with nitrogen gas over a period of 1 h. This purge time was enough to consider almost complete DO depletion in the solution as previously reported by Ghauch et al. [33]. The results showed a net decrease in  $k_{\text{obs}}$  by almost half of its value obtained under oxic conditions e.g.  $(0.817 (\pm 0.41) \times 10^{-1} \text{ min}^{-1})$  vs  $(1.73 (\pm 0.04) \times 10^{-1} \text{ min}^{-1})$  (Fig. 4). In fact, powerful ROS such as  $\text{O}_2^-$  might be formed and contribute greatly to the oxidation of organic compounds toward mineralization [62]. Fig. 5S presents the use of chloroform as a superoxide quencher [63]. Results showed that slower degradation is obtained in the presence of chloroform for the first 6 min after which degradation rate increases possibly due to the generation of chlorine-based active radicals that might contain in addition of chlorine, carbon and hydrogen. Accordingly, these generated chlorine-based radicals are different than chlorine radicals produced from chloride ions in water in terms of chemical reactivity (Section 3.4.2). Thus,  $\text{O}_2^-$  is expected to be formed in the UV<sub>254nm</sub>/PS system studied.

### 3.5. Case of spring, sea and wastewater

Since pharmaceutical effluents are in general mixed to different water matrices upon their discharge in the surroundings, the effectivity of the degradation process was studied in real water samples. Spring, sea and wastewater samples were taken from 33°44'17.9"N

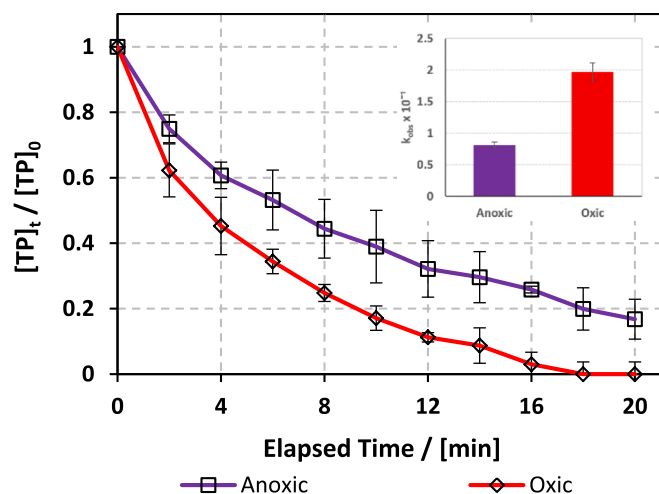


Fig. 4. Effect of the presence of dissolved oxygen on TP degradation in UV<sub>254</sub>/PS system. Anoxic conditions are obtained upon N<sub>2(g)</sub> bubbling for 20 min. Oxidic conditions are obtained without any N<sub>2</sub> bubbling with [DO] = 8 mg L<sup>-1</sup> at room temperature. Experimental conditions: [TP]<sub>0</sub> = 10 mg L<sup>-1</sup> and [PS]<sub>0</sub> = 0.25 mM. Error bars are calculated as  $\frac{ts}{\sqrt{n}}$ , where absent bars fall within the symbols. The inset shows k<sub>obs</sub> values for anoxic and oxidic conditions.

35°34'12.5"E, 33°54'11.1"N 35°28'44.8"E and 33°54'08.2"N 35°29'05.0"E locations, respectively. These samples were spiked with an appropriate volume of TP and PS stock solutions so as to obtain the following starting concentrations: [PS]<sub>0</sub> = 0.25 mM and [TP]<sub>0</sub> = 10 mg L<sup>-1</sup>. As it can be noticed from the obtained results (Fig. 5a,b), TP degradation was hindered in the three water matrices tested, where k<sub>obs</sub> decreased from 1.73 (±0.04) × 10<sup>-1</sup> min<sup>-1</sup> in DI matrix to 8.5 (±0.7) × 10<sup>-2</sup> min<sup>-1</sup>, 7.2 (±0.8) × 10<sup>-2</sup> min<sup>-1</sup>, and 6.9 (±0.9) × 10<sup>-3</sup> min<sup>-1</sup> in sea, spring and wastewater matrices, respectively. k<sub>obs</sub> was the lowest in the case of wastewater, where total and fecal coliforms, chlorides, sulfates, bicarbonates, chemical oxygen demand (COD) and turbidity were the highest. This decrease in the oxidation rate can be explained by the competing reactions occurring in solution, where PS would react with organic compounds present in the medium leading to a decrease in its concentration and therefore its conversion rate into SO<sub>4</sub><sup>-</sup> participating in the TP oxidative degradation reaction. Another factor that most probably contributed to the decrease in the degradation rate constant of the oxidative reaction is the drop in the penetration capacity of the UV-254 nm rays reaching the entire solution due to increased turbidity. This is in accordance with previous work done on wastewater by Ghach group on the degradation of chloramphenicol and ketoprofen in similar UV/PS systems, where in both cases, degradation in wastewater had the lowest rate [19,21]. As

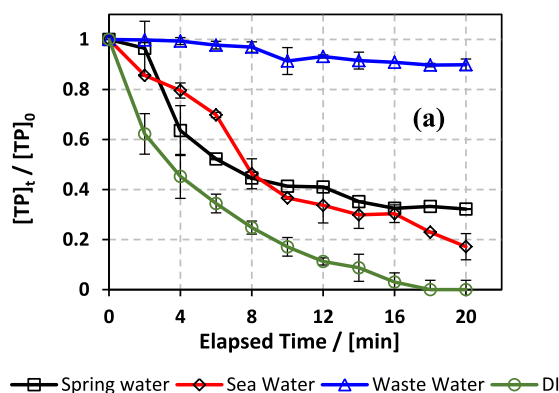


Fig. 5. (a) Degradation of TP in real water samples: spring, sea and wastewater, and (b) calculated degradation rate constants k<sub>obs</sub>. Error bars are calculated as  $\frac{ts}{\sqrt{n}}$ , where absent bars fall within the symbols.

for sea and spring water, k<sub>obs</sub> were very close which can be explained by the minor effect of chloride ions as demonstrated in the previous section. One can also notice from Table 2 that TC and TFC decreased in sea water upon treatment due most probably to the use of the UV-254 nm germicidal lamps, in addition to the possible effect of PS oxidation acting on the various micro-organisms present. However, in the case of wastewater, TC and TFC were still significantly present even after treatment (Table 2). Thus, when dealing with complex polluted water media, AOPs are more significant for implementation as a tertiary treatment technique, where fewer particles are present in the medium and limited competing reactions are favored so that oxidation is thus more effective [64].

### 3.6. Effectivity of sulfate and hydroxyl radicals

Upon activation of PS in water, SO<sub>4</sub><sup>-</sup> as well as HO<sup>•</sup> are expected to be formed. To test for relative effectiveness of the SO<sub>4</sub><sup>-</sup> and HO<sup>•</sup> produced on TP degradation, quenching experiments were performed upon adding methanol (MeOH) and *tert*-Butyl-alcohol (TBA) separately. Experiments were conducted in TP solutions (10 mg L<sup>-1</sup>) with MeOH and TBA concentrations of about 100 mM which is 400 times greater than the concentration of PS used (e.g. 0.25 mM) to ensure proper quenching of radicals. Eqs. (20)–(23) [19] and the analyses of the reaction rate ratio  $\left(\frac{k_{HO^{\bullet}}}{k_{SO_4^{\bullet-}}}\right)$  show that MeOH and TBA are respectively 88 and 1,500 times kinetically more reactive toward HO<sup>•</sup> than SO<sub>4</sub><sup>-</sup>, thus it can be said that TBA mainly quenches OH<sup>•</sup> while MeOH quenches both mentioned radicals.

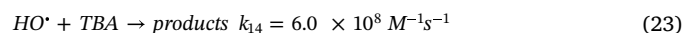
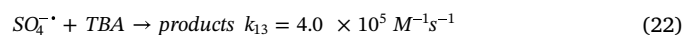
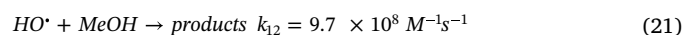
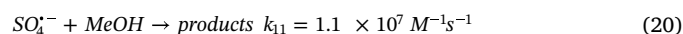
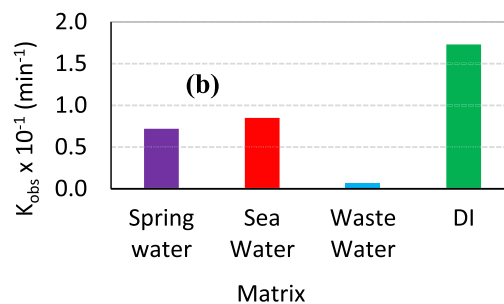


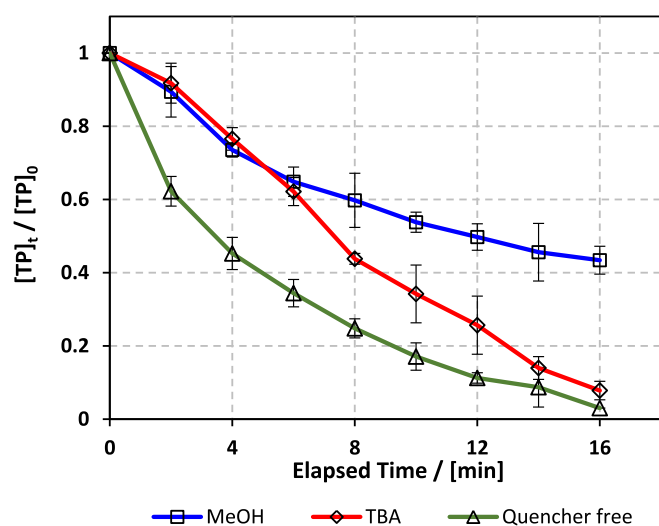
Fig. 6 and Table 1 show clearly that the spiked scavengers decreased the rate constants of TP oxidation reaction. For example, k<sub>obs</sub> decreased from 1.73 (±0.04) × 10<sup>-1</sup> min<sup>-1</sup>, to 1.5 (±0.01) × 10<sup>-1</sup> min<sup>-1</sup> and 5.4 (±0.3) × 10<sup>-2</sup> min<sup>-1</sup> for the cases of no quencher, TBA and MeOH, respectively (Table 1). The % degradation at t = 16 min was 95% for the case of no quencher and decreased to 92% and 57% for the cases of TBA and MeOH, respectively.

Tracking the % contribution of every radical and considering Eqs. (20)–(23), SO<sub>4</sub><sup>-</sup> is shown to be the main contributor (% contribution average ≥ 84%) to the oxidation process in the medium. In fact, SO<sub>4</sub><sup>-</sup> is the prominent contributor in the first 6 min which resulted in a similar degradation trend for the case of TBA and MeOH at the beginning of the reaction. After that, HO<sup>•</sup> contribution increases from null to reach



**Table 2**Physical parameters of the natural water matrices before and after treatment in UV<sub>254</sub>/PS system. Experimental conditions: [TP]<sub>0</sub> = 10 mg L<sup>-1</sup> and [PS]<sub>0</sub> = 0.25 mM.

Parameters	units	Spring Water		Sea Water		Waste Water	
		Before treatment	After treatment	Before treatment	After treatment	Before treatment	After treatment
pH	–	7	6.86	8	7.45	8.2	7.93
Total Coliforms	CFU <sup>a</sup>	NA	NA	76	NA	TNTC <sup>c</sup>	TNTC
Fecal Coliforms		NA	NA	4	NA	TNTC	TNTC
Turbidity	NTU <sup>b</sup>	0.63	0.38	1	0.17	95	69
TSS	mg L <sup>-1</sup>	9	2	88	126	425	38
TDS		350	332	32,500	47,400	4400	3840
Sulfate		16	30	3500	3500	420	490
Chloride		42.6	1.85	25,250	21,500	3375	2090
Bicarbonate		230	210	177	156	280	250
COD <sup>d</sup>		132	43	970	930	1106	426

<sup>a</sup> Colony forming unit.<sup>b</sup> Nephelometric turbidity unit.<sup>c</sup> Too numerous to count.<sup>d</sup> Chemical oxygen demand.

**Fig. 6.** Identification of the reactive species for TP degradation in UV<sub>254</sub>/PS system. Time course degradation of TP in the absence and in the presence of MeOH and TBA quenchers. Experimental conditions: [MeOH] = [TBA] = 100 mM, [TP]<sub>0</sub> = 10 mg L<sup>-1</sup>, and [PS]<sub>0</sub> = 0.25 mM. Error bars are calculated as  $\frac{\sigma}{\bar{x}}$ , where absent bars fall within the symbols.

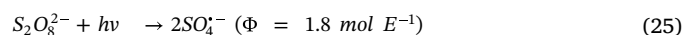
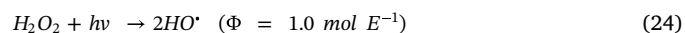
≤ 28% at t = 16 min. The method used to determine the % contribution of radicals is explained in Text S4, where it utilizes and compares the values of  $\frac{[TP]_t}{[TP]_0}$  in cases of MeOH and TBA presence.

This can be related to the initial pH of the reaction medium, where pH<sub>i</sub> was acidic (pH<sub>i</sub> = 5.3, 6.3 and 5.4 for quencher-free, MeOH and TBA experiments, respectively) which inhibits the formation of HO<sup>•</sup> [34]. HO<sup>•</sup> is known to perform as H<sup>•</sup> abstractor, while SO<sub>4</sub><sup>•-</sup> is known to act selectively by electron transfer (ET) [65]. As a result, one can deduce that TP, in the tested case, is mainly degraded by ET. This can be explained by the presence of the atoms N and O in TP prone to ET reactions. SO<sub>4</sub><sup>•-</sup> was the main reactive species in several other AOPs studies utilizing either UV<sub>254</sub>/PS [25,44,48] or heat/PS [47,50,51,53–55] systems especially in slightly acidic media.

### 3.7. Comparative study: UV<sub>254</sub>/H<sub>2</sub>O<sub>2</sub>; UV<sub>254</sub>/PS and UV<sub>254</sub>/H<sub>2</sub>O<sub>2</sub>/PS systems

In order to assess the performance of the PS-based AOP systems tested throughout this work, additional experiments were done so as to evaluate the oxidation power of such a system in the presence of H<sub>2</sub>O<sub>2</sub> oxidant alone ([H<sub>2</sub>O<sub>2</sub>] = 0.25 mM) or in combination with PS

([H<sub>2</sub>O<sub>2</sub>] = [PS] = 0.125 mM) at [TP]<sub>0</sub> = 10 mg L<sup>-1</sup>. Fig. 6Sa,b shows that systems utilizing (H<sub>2</sub>O<sub>2</sub> + PS) or H<sub>2</sub>O<sub>2</sub> alone were slightly better performing than PS-alone system. In fact homolytic cleavage of H<sub>2</sub>O<sub>2</sub> and PS by UV-C activation allows the formation of two SO<sub>4</sub><sup>•-</sup> and two HO<sup>•</sup> respectively, and the consecutive formation of HO<sup>•</sup> from SO<sub>4</sub><sup>•-</sup> is pH dependent and more prominent at basic pH (Eq. (4)) [34]. Although a higher quantum yield is expected for S<sub>2</sub>O<sub>8</sub><sup>2-</sup> activation (Eqs. (24) and (25)) [22,66], greater effectivity of H<sub>2</sub>O<sub>2</sub> system than that of PS system may be explained by the higher effectivity of HO<sup>•</sup> in the degradation process. For the case of (H<sub>2</sub>O<sub>2</sub> + PS) system, high k<sub>obs</sub>, close to k<sub>obs</sub> obtained for H<sub>2</sub>O<sub>2</sub> system was found due to the formation of both effective SO<sub>4</sub><sup>•-</sup> and HO<sup>•</sup> where the resulting pH<sub>f</sub> is higher than that of PS case allowing HO<sup>•</sup> to be more prominent. Thus, more HO<sup>•</sup> is formed in the hybrid case than in the case of PS alone. The pH<sub>i</sub> in the current three studied cases ranged between 5.2 and 5.7. For this same pH range, Yang et al. (2017) [67] also found H<sub>2</sub>O<sub>2</sub> to be more effective than PS in degrading sulfamethoxazole, however, at around neutral pH, PS was more effective in its degradation. Olmez-Hanci et al. [34] also obtained larger k<sub>obs</sub> for H<sub>2</sub>O<sub>2</sub>/UV-C (0.175 ± 0.003 min<sup>-1</sup>) than for PS/UV-C (0.106 ± 0.001 min<sup>-1</sup>) system in the degradation of 48 mg L<sup>-1</sup> aqueous phenol solution at fixed acidic pH value (pH = 3.0). Yang et al. (2017) [67] and Yang et al. (2019) [68] showed that efficiency of H<sub>2</sub>O<sub>2</sub> is not significantly affected by pH change, whereas, PS degradation activity decreases at extreme acidic pH and in basic media as well. Thus, the preference of the oxidant to be used would depend on the pH of the corresponding medium, as well as the cost and stability of the oxidant. A comparison between the two oxidants shows that H<sub>2</sub>O<sub>2</sub> degrades into water and oxygen, whereas PS results in sulfate ions in the treated water which poses an environmental concern. On the other side, PS shows an advantage over H<sub>2</sub>O<sub>2</sub> in terms of transportation, storage, shelf-life and requiring much less safety conditions. The sulfates produced, when utilizing PS, can be removed by well-known methods, such as ion exchange and nanofiltration [69], or else they can stay in the treated effluent and will get diluted once discharged into the sea containing around 2,700 mg L<sup>-1</sup> SO<sub>4</sub><sup>2-</sup> [70]. Even for the use of high concentration of PS, e.g. 25 mM as it is the case for TP effluent (Section 3.9.1), the maximum produced sulfate concentration will not exceed 4,800 mg L<sup>-1</sup> for a small treated volume that is potent for further dilution upon discharge.



### 3.8. Mass spectrometry and suggested mechanism

HPLC/MS(-ESI) analysis was done on samples taken at t = 0, 6, 12

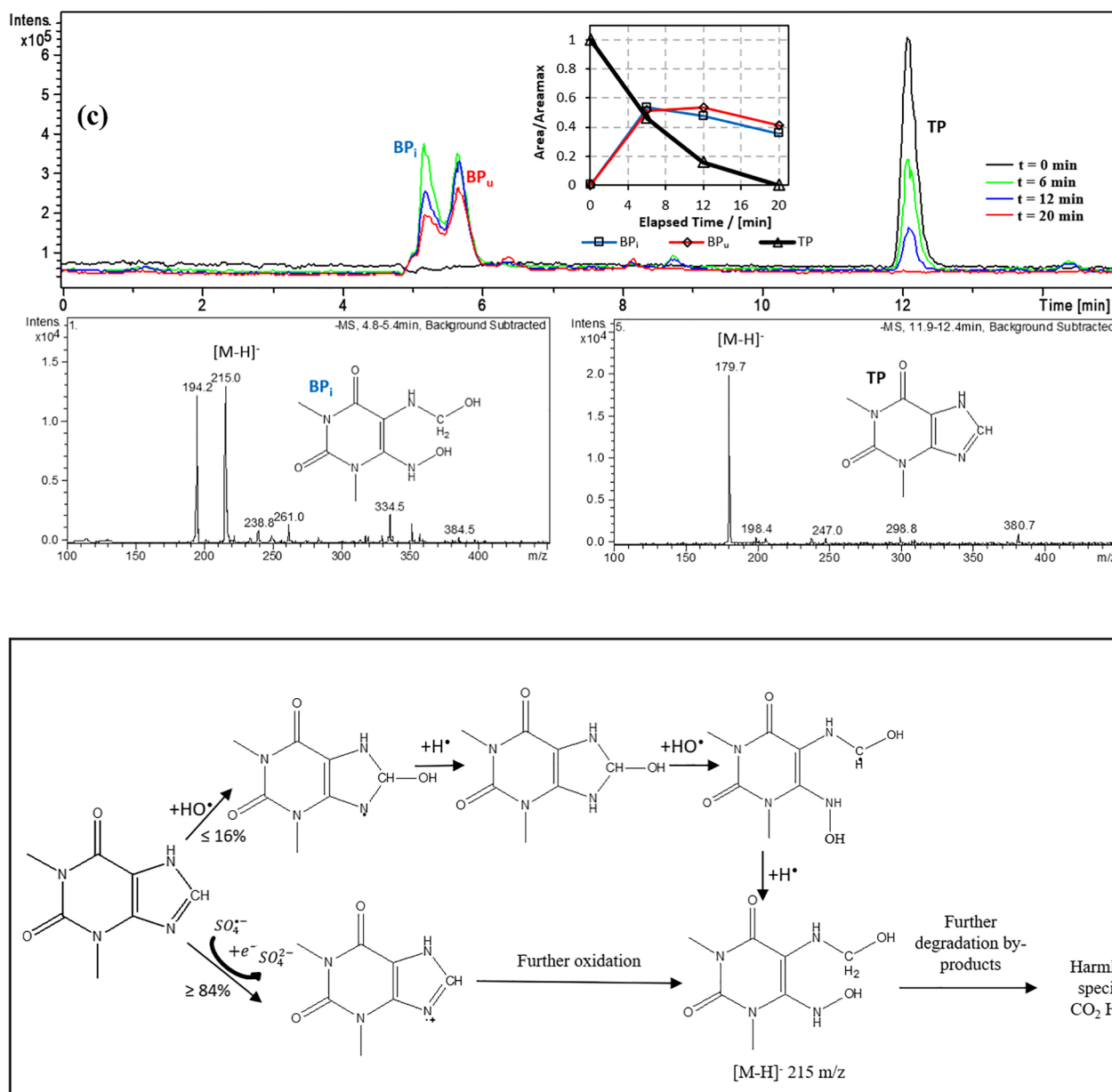


**Fig. 7.** (a) (-) ESI LC-MS total ion chromatogram of TP degradation at different reaction times in UV<sub>254</sub>/PS system, containing a graph showing relative peak areas of the identified and unidentified by-products (BP<sub>i</sub> and BP<sub>u</sub>), in addition to TP. (b) Mass spectrum of degradation by-product at  $R_t = 5.2$  min and of TP ( $R_t = 12.2$  min). (c) Proposed TP degradation mechanism by  $\text{SO}_4^{\bullet-}$  and  $\text{HO}^\bullet$ . Experimental conditions:  $[\text{TP}]_0 = 10 \text{ mg L}^{-1}$  and  $[\text{PS}]_0 = 0.25 \text{ mM}$ .

and 20 min for  $[\text{TP}]_0 = 10 \text{ mg L}^{-1}$  and  $[\text{PS}]_0 = 0.25 \text{ mM}$ . The total ion chromatograms (TIC) obtained showed a main peak corresponding to TP at  $R_t = 12.2$  min, in addition to two peaks corresponding to an identified (BP<sub>i</sub>) and an unidentified (BP<sub>u</sub>) by-product observed at  $R_t = 5.2$  and  $5.8$  min, respectively as it can be depicted in Fig. 7a. TP peak showed total degradation where a maximum peak area is observed at  $t = 0$  min to vanish completely after 20 min of reaction time (Fig. 7a). For both BP<sub>i</sub> and BP<sub>u</sub> no peaks were initially observed however maximum detector responses were obtained at 6 min of reaction to decrease again with time as shown in the inset of Fig. 7a. Thus, by-products are successively formed and degraded in the UV<sub>254</sub>/PS system. This might be due to direct photolysis or to the oxidative role of produced  $\text{HO}^\bullet$  and/or  $\text{SO}_4^{\bullet-}$  in the reactive medium. The mass spectrum of BP<sub>i</sub> showed two main peaks at  $m/z = 194.2$  and  $215.0$ . The former peak is a non-identified fragment while the latter corresponded to the identified transformation TP by-product BP<sub>i</sub> at its  $[\text{M-H}]^-$  molecular ion (Fig. 7b)). The mass spectrum of TP showed a major peak of  $m/$

$z = 179.7$  corresponding to TP molecular ion of  $[\text{M-H}]^-$ . The suggested degradation mechanism is presented in Fig. 7c, showing probable initiation of the degradation process by the attack of either  $\text{HO}^\bullet$  or  $\text{SO}_4^{\bullet-}$  on TP molecule. As previously suggested, TP has more chances to undergo  $\text{SO}_4^{\bullet-}$  attack with a contribution of about 86% at the beginning of the oxidation reaction as shown in Section 3.6. Both attacks result in the formation of an unstable molecule, possessing an unpaired electron ready for rapid reaction to reach stability. Hydroxyl additions might occur increasing thereby the internal energy of the molecule more specifically the five-membered ring for potential ring opening. In fact, it is well known that five-membered rings are less stable than six-membered rings and in the case of TP, the molecule showed some hindrance in its six-membered ring part leaving structure changes at the five-member part. The transformation products are not neutral in the reactive medium and can undergo further oxidation toward full mineralization as reported in previous work using comparable UV<sub>254</sub>/PS systems [19,21]. The formed species also contribute to a drop in the

solution's pH ( $\Delta\text{pH} = 1.6$ ,  $\text{pH}_f = 3.8$ ) affecting thereby all possible oxidation reactions in the reactive medium. Such a drop in pH could be attributed to low molecular weight acids that are the ultimate organic molecules to be formed in a common AOP system just before total mineralization [71,72].

### 3.9. Case study: Pharmaceutical effluent

#### 3.9.1. Optimization of $[\text{PS}]_0$ for efficient degradation

In order to assess the applicability of the studied  $\text{UV}_{254}/\text{PS}$  system on real pharmaceutical effluents, a field study was conducted. Wastewater was collected from a Lebanese pharmaceutical production plant that produces a syrup containing TP in addition to several excipients. All ingredients are added to a 1000 L 316 SS L mixing container, after which the mixture is pumped through a filter press into a 100 L 316 SS L container. Wastewater samples were collected from the washing effluent obtained upon cleaning the 1000 L 316 SS L mixing container and the filter press (Fig. 7Sa,c). DI water is used in the pharmaceutical factory for cleaning and washing all utensils used for any drug production including the mixing reactors. The resulting wastewater mixture was analyzed and showed high concentration of TP of about  $160 \text{ mg L}^{-1}$  supposed to be discarded directly into the municipal sewer system without prior treatment

The pharmaceutical effluent mixture was treated using the  $\text{UV}_{254}/\text{PS}$  system with  $[\text{PS}]_0 = 25, 50, 75$  and  $100 \text{ mM}$ . Results showed that almost total degradation was reached in the four cases, with minor decrease in the efficiency of the oxidation reaction for the lower  $[\text{PS}]_0$  used e.g.  $25 \text{ mM}$  (Fig. 8). As it can be seen, the degradation rate constant  $k_{\text{obs}}$  decreased by almost 57% from  $2.20 (\pm 0.08) \times 10^{-2} \text{ min}^{-1}$  for  $[\text{PS}]_0 = 100 \text{ mM}$  to  $1.4 (\pm 0.1) \times 10^{-2} \text{ min}^{-1}$  for  $[\text{PS}]_0 = 25 \text{ mM}$  (Table 3).

The  $\text{UV}_{254}/\text{PS}$  treatment caused a drop in pH, with a maximum of  $\Delta\text{pH} = 2.35$  (Eqs. (2) and (3)). The COD value of the effluent was  $28000 \text{ mg L}^{-1}$  which is typical of a highly charged industrial effluent. After treatment, COD values in cases of  $[\text{PS}]_0 = 75$  and  $100 \text{ mM}$  were corrected using calibration curve method in order to eliminate the overestimation caused by PS remained in the solution (Text S5, Table S5)[73,74]. The treatment showed a decrease in the biological oxygen demand ( $\text{BOD}_5$ ) proportional to  $[\text{PS}]_0$  used demonstrating that PS is effective in targeting organic contaminants (Table 3). The addition of high concentration of sodium persulfate salt resulted in a sharp increase

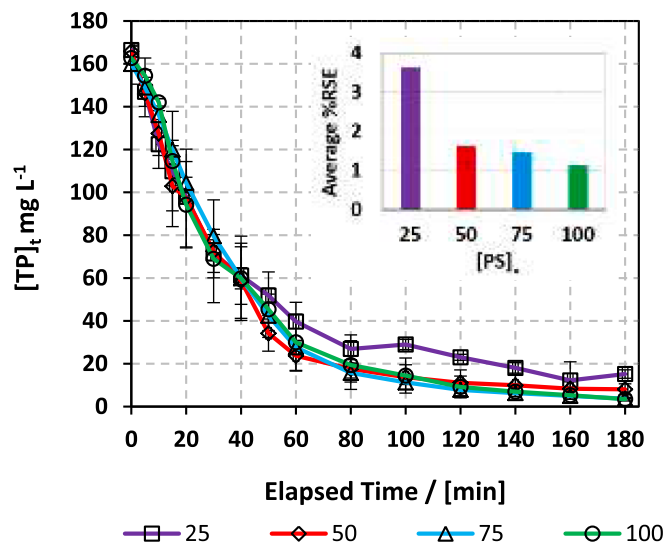


Fig. 8. Degradation of TP in a real pharmaceutical effluent. Experimental conditions:  $[\text{TP}]_0 = 160 \text{ mg L}^{-1}$  and  $[\text{PS}]_0 = 25\text{--}100 \text{ mM}$ . The inset shows the average % RSE values determined at each PS concentration. Error bars are calculated as  $\frac{ts}{\sqrt{n}}$ , where absent bars fall within the symbols.

Table 3

Physical parameters of the pharmaceutical effluent before and after treatment in the  $\text{UV}_{254}/\text{PS}$  system at initial ( $t = 0 \text{ min}$ ) and final ( $t = 180 \text{ min}$ ) time. Experimental conditions:  $[\text{TP}]_0 = 160 \text{ mg L}^{-1}$  and  $[\text{PS}]_0 = 25\text{--}100 \text{ mM}$ .

[PS] mM	0	25	50	75	100
$k_{\text{obs}} \text{ min}^{-1} (\times 10^{-2})$	–	$1.4 (\pm 0.1)$	$1.8 (\pm 0.1)$	$2.2 (\pm 0.1)$	$2.20 (\pm 0.08)$
$\text{pH}_i/\text{pH}_f$	–	3.43/1.53	3.43/1.15	4.15/1.89	4.15/1.80
$\text{COD}^a (\text{mg L}^{-1})$	28,000	27,390	27,130	23,824	22,474
$\text{BOD}_5^b (\text{mg L}^{-1})$	11,505	10,620	10,020	7530	8850
$\text{TDS}^c (\text{g L}^{-1})$	0.394	6.095	8.578	14.06	17.47

<sup>a</sup> Chemical oxygen demand.

<sup>b</sup> Biological oxygen demand in five days.

<sup>c</sup> Total dissolved solid.

in the total dissolved solids with the increase in  $[\text{PS}]_0$  (Table 3).

Moreover, the [PS] was tracked throughout the reaction time and the % RSE was determined for the four studied cases following Eq. (26). The RSE is defined as the ratio of the number of moles of the degraded organic contaminant divided by the number of moles of oxidant (PS) consumed in the process.

$$\% \text{ RSE} = \frac{n(\text{TP})_{\text{degraded}}}{n(\text{PS})_{\text{consumed}}} \times 100 \quad (26)$$

The % RSE showed the highest value of 3.7% at  $[\text{PS}]_0 = 25 \text{ mM}$  (Fig. 8). Thus, this concentration is considered the optimum case to adopt for the degradation of high TP's content effluent e.g.  $160 \text{ mg L}^{-1}$ . A higher % RSE (52%) was obtained by Ghauch et al. upon degradation of Chloramphenicol (CAP) in DI medium in a similar  $\text{UV}_{254}/\text{PS}$  systems [19]. This observation is not surprising for three reasons: (1) the lesser is the concentration of PS used in the medium (0.25 mM for CAP against 25 mM for TP), the greater is the % RSE obtained as previously demonstrated; (2) competitive reactions of PS with most of the excipients (e.g. sorbitol, potassium sorbate, ethanol, vanillin and saccharine, as provided by manufacturer) can cause a decrease in the production of  $\text{SO}_4^{\cdot -}$  (because of radical quenching with ethanol for example) and in the efficiency of  $\text{SO}_4^{\cdot -}$  to only hit the selected TP probe; and (3) direct photolysis which is not significant in the current case (~10% on average, Fig. 1) compared to that of CAP (65%).

#### 3.9.2. Economic feasibility

Economic feasibility was assessed utilizing electric energy per order ( $E_{\text{EO}}$ ) and the prices of chemicals used.  $E_{\text{EO}}$  ( $\text{kWh}/\text{m}^3/\text{order}$ ) is defined as the electric energy in kilowatt hours required to degrade contaminants by one order of magnitude, for example from  $10 \text{ mg L}^{-1}$  to  $1 \text{ mg L}^{-1}$ , in one cubic meter of contaminated air or water, and is calculated using Eq. (27) for a batch system [75].

$$E_{\text{EO}} = \frac{P \times t \times 1000}{V \times \log(C_i/C_f)} \quad (27)$$

where P is the power supplied to the system in kW, t is the duration of treatment in hour, V is the volume treated in L,  $C_i$  and  $C_f$  are the respective initial and final concentrations, and 1000 is a conversion factor from L to  $\text{m}^3$ .

To simplify Eq. (27), the first-order reaction rate is used Eq. (28). Changing unit of t and substitution of Eq. (28) in Eq. (27), the following simplification is done (Eqs. (28)–(30)).

$$\log \frac{C_i}{C_f} = 0.4343 \times k_{\text{obs}} \times t \quad (28)$$

$$E_{\text{EO}} = \frac{P \times t \times 1000}{V \times 0.4343 \times k_{\text{obs}} \times t \times 60} \quad (29)$$

$$E_{\text{EO}} = \frac{38.4 \times P}{V \times k_{\text{obs}}} \quad (30)$$

**Table 4**  
Total system cost based on electricity price rates in Lebanon and in the US.

E <sub>EO</sub> (kWh/m <sup>3</sup> /order)	Electricity cost (\$/m <sup>3</sup> )		Reagent price (\$/m <sup>3</sup> )	Total cost (\$/m <sup>3</sup> )	
	Lebanon	US		Lebanon	US
75	12.8	5.35	11.9	24.7	17.2

In the simplified Eq. (30), P is in kW, V in L,  $k_{obs}$  in  $\text{min}^{-1}$ , and EEO is in  $\text{kWh}/\text{m}^3/\text{order}$  [75]. The total cost is calculated for the case of  $[\text{PS}]_0 = 25 \text{ mM}$  since it was chosen as the optimum concentration yielding almost full TP degradation in the pharmaceutical effluent. In our studied UV<sub>254</sub>/PS system, each 0.4 L reactor used required an 11 Watts lamp.  $k_{obs}$  for the case of  $[\text{PS}]_0 = 25 \text{ mM}$  is  $1.4 (\pm 0.1) \times 10^{-2} \text{ min}^{-1}$ . Thus, the EEO for the studied case is  $75 \text{ kWh}/\text{m}^3/\text{order}$ . Finally, in order to determine the total cost of the proposed pharmaceutical effluent treatment in batch system, Eq. (31) was used as it follows:

$$\text{Total system cost} (\$/\text{m}^3) = \text{Electrical Energy Cost} + \text{Reagent Cost} \quad (31)$$

The electrical energy cost is estimated based on the actual electricity cost in Lebanon and in the United States. In the former, Electricité du Liban (EDL) average rate of 255 LBP/kWh is equivalent to 0.169 \$/kWh at the current conversion rate [76,77], while in the latter, the average electricity cost for the industrial sector is about 0.0709 \$/kWh. As for reagent cost, it is calculated using wholesale prices available on-line through the local distributors (Table S4). The total system cost is presented in detail in Table 4, where, based on prices of electricity in the US, a total of 17.2 \$ is enough to treat  $1 \text{ m}^3$  of a highly charged pharmaceutical effluent with the reagent price being the main contributor to the total price. If the treatment is to be done in Lebanon, however, it is expected to cost more ( $24.7\% \text{ m}^{-3}$ ) since electricity prices are higher.

### 3.9.3. Effect of successive PS spiking

The effect of successive versus simultaneous addition of PS was tested in order to find the better way of improving the oxidation process by avoiding potential radical-radical quenching that might decrease the reaction efficiency. The results presented in Text S6 and Fig. 8S of supplementary information showed the same outcomes in terms of complete degradation of TP along with total PS consumption. Accordingly, oxidation reaction can be performed in solutions of high concentration and ionic strength through elevated [PS] and without decreasing significantly the degradation yield of the pharmaceutical compounds in question. Moreover, one can notice that the % RSE, calculated for each cycle separately, was about 3.6%. However, it dropped with every cycle to reach 0.6% in the fifth cycle, which can be explained by the competitive reactions between active radicals e.g.  $\text{SO}_4^{\cdot-}$ ,  $\text{HO}^{\cdot}$  to degrade the accumulated by-products versus initial [TP] present in solution.

### 3.9.4. Test of the system robustness

The robustness of the UV<sub>254</sub>/PS system was tested upon spiking the reaction medium with concentrated effluent solution, where lower degradation was observed with each spiking accompanied with lesser % RSE as depicted in Fig. 8S. For example, a drop in the % RSE from 4.5 to 0.5 after 3 h of reaction was noticed with 90% of the initial [PS] consumed in the first cycle of 60 min. Accordingly, it is suggested that the system used is thus of low tolerance to major fluctuations in effluent concentration.

As a result, one can deduce that in cases of varying and increasing effluent concentrations upon characterization, it is recommended that PS be spiked successively (Section 3.9.3) with [PS] range consistent with that of [TP] fluctuation. More details are provided in Text S6 of supplementary information.

## 4. Conclusions

TP degradation was tested in an assembled UV<sub>254</sub>/PS lab scale batch system for simulated and real concentrated industrial effluents. The effect of various experimental parameters on TP degradation was studied. Results showed that UV<sub>254</sub> alone could not efficiently degrade TP through photolysis only phenomenon, while the addition of  $[\text{PS}]_0 = 0.25 \text{ mM}$  totally degraded  $[\text{TP}]_0 = 10 \text{ mg L}^{-1}$  within 20 min following a pseudo-first order reaction kinetics ( $k_{obs} = 0.173 (\pm 0.004) \text{ min}^{-1}$ ). The degradation process was inhibited in acidic and basic media, while neutral pH showed improved degradation ( $k_{obs} = 0.40 (\pm 0.03) \text{ min}^{-1}$ ). Bicarbonate as well as chloride presence had minimal effect on TP degradation rate. In spring, sea and wastewater matrices TP showed slower degradation than that in DI confirming thereby the necessity of treating pharmaceutical factory effluents independently before mixing them with natural water. The studied system was successfully applied to treat TP in a real industrial effluent highly charged in TP (e.g.  $160 \text{ mg L}^{-1}$ ) dissolved in a DI water matrix. The UV<sub>254</sub>/PS system resulted in the complete degradation of TP in a real pharmaceutical production facility effluent over 180 min however using 25 mM of PS and reaching an optimum % average RSE of about 3.7%. The economic feasibility study estimated the cost of the chosen AOP to be close to  $17.2 \text{ \$ m}^{-3}$  in highly charged effluents. The results showed also that adding PS to the effluent mixture simultaneously at  $t = 0 \text{ min}$  or successively over the reaction course (e.g. 180 min) resulted in full TP degradation accompanied with a total consumption of the initial PS added. However, it was demonstrated that the system was not robust against [TP] fluctuation, where a sudden increase in effluent concentration requires a relative increase of [PS] added. It was concluded that oxidant dosage should be determined based on temporal monitoring of the pharmaceutical active ingredient concentration under degradation. Based on ROS quenching experiments, it was demonstrated that the UV<sub>254</sub>/PS system put in advance  $\text{SO}_4^{\cdot-}$  as the main contributors to TP degradation especially at the beginning of the oxidation reaction. Although full TP degradation was reached, however LC/MS analysis depicted the presence of non-persistent TP transformation products that vanished with time. Finally, this work has reported for the first time the feasibility of the UV<sub>254</sub>/PS systems in degrading persistent PAIs at very high concentration in batch systems and opened the way toward continuous additional investigation for effluent treatment in a continuous system.

## Acknowledgements

This research was funded in part by the Lebanese National Council for Scientific Research (Award Number 103250), the K Shair CRSL fund (Award Number 103191), and the University Research Board (Award Number 103186) of the American University of Beirut and USAID-Lebanon through The National Academy of Sciences under PEER project 5-18 (Award number 103262). Prof. Antoine Ghauch greatly appreciates the help of M. Ramez Lotfi, the GM of MEPHICO, allowing access to the production line for samples collection. The author is thankful to Joan Younes, Samer Khalil, Simon Al-Ghawry, and Boutros Sawaya for their technical assistance and the personnel of the K. Shair CRSL for their kind help. The author is also grateful to graphic designer Zaynab Mayladan for her help in drawing the graphical abstract.

## Appendix A. Supplementary data

Supplementary data to this article can be found online at <https://doi.org/10.1016/j.cej.2019.122478>.

## References

- [1] K. Noguera-Oviedo, D.S. Aga, Lessons learned from more than two decades of research on emerging contaminants in the environment, J. Hazard. Mater. 316 (2016)

- 242–251, <https://doi.org/10.1016/j.jhazmat.2016.04.058>.
- [2] R. Hirsch, T. Ternes, K. Haberer, K.-L. Kratz, Occurrence of antibiotics in the aquatic environment, *Sci. Total Environ.* 225 (1999) 109–118, [https://doi.org/10.1016/S0048-9697\(98\)00337-4](https://doi.org/10.1016/S0048-9697(98)00337-4).
- [3] W.W. Buchberger, Current approaches to trace analysis of pharmaceuticals and personal care products in the environment, *J. Chromatogr. A* 1218 (2011) 603–618, <https://doi.org/10.1016/j.chroma.2010.10.040>.
- [4] I. American, Society of health-system pharmacists, Theophylline (2017).
- [5] C.A. Shively, S.M. Tarka, Methylxanthine composition and consumption patterns of cocoa and chocolate products, *Prog. Clin. Biol. Res.* 158 (1984) 149–178 <http://europepmc.org/abstract/MED/6396642>.
- [6] D.D. Tang-Liu, R.L. Williams, S. Riegelman, Disposition of caffeine and its metabolites in man, *J. Pharmacol. Exp. Ther.* 224 (1983) 180–185 <http://jpet.aspetjournals.org/content/224/1/180>.
- [7] M.E. Rybak, M.R. Sternberg, C.-I. Pao, N. Ahluwalia, C.M. Pfeiffer, Urine excretion of caffeine and select caffeine metabolites is common in the US population and associated with caffeine intake, *J. Nutr.* 145 (2015) 766–774.
- [8] T. Heberer, Occurrence, fate, and removal of pharmaceutical residues in the aquatic environment: a review of recent research data, *Toxicol. Lett.* 131 (2002) 5–17, [https://doi.org/10.1016/S0378-4274\(02\)00041-3](https://doi.org/10.1016/S0378-4274(02)00041-3).
- [9] J. Doummar, K. Nödler, T. Geyer, M. Sauter, Assessment and Analysis of Micropollutants 2010–2011 n.d.
- [10] K.V. Blake, A. Neims, D. Nickerson, K.L. Massey, L. Hendeles, Relative efficacy of phenytoin and phenobarbital for the prevention of theophylline-induced seizures in mice, *Ann. Emerg. Med.* 17 (2005) 1024–1028, [https://doi.org/10.1016/s0196-0644\(88\)80439-6](https://doi.org/10.1016/s0196-0644(88)80439-6).
- [11] J.D. Journey, T.P. Bentley, Theophylline Toxicity, StatPearls Publishing, Treasure Island (FL), n.d. <http://europepmc.org/books/NBK532962>.
- [12] S.M.Z. Connor, Richard, Angela Renata, Cordeiro Ortigara, Engin Koncagül, Stefan Uhlenbrook, Birguy M. Lamizana-Diallo, The United Nations World Water Development Report (2017), 2017.
- [13] Y. Luo, W. Guo, H.H. Ngo, L.D. Nghiem, F.I. Hai, J. Zhang, S. Liang, X.C. Wang, A review on the occurrence of micropollutants in the aquatic environment and their fate and removal during wastewater treatment, *Sci. Total Environ.* 473–474 (2014) 619–641, <https://doi.org/10.1016/j.scitotenv.2013.12.065>.
- [14] R. Liang, S. Luo, F. Jing, L. Shen, N. Qin, L. Wu, A simple strategy for fabrication of Pd@MIL-100(Fe) nanocomposite as a visible-light-driven photocatalyst for the treatment of pharmaceuticals and personal care products (PPCPs), *Appl. Catal. B Environ.* 176–177 (2015) 240–248, <https://doi.org/10.1016/j.apcatb.2015.04.009>.
- [15] I. Kim, N. Yamashita, H. Tanaka, Photodegradation of pharmaceuticals and personal care products during UV and UV/H<sub>2</sub>O<sub>2</sub> treatments, *Chemosphere* 77 (2009) 518–525, <https://doi.org/10.1016/j.chemosphere.2009.07.041>.
- [16] I. Kim, H. Tanaka, Photodegradation characteristics of PPCPs in water with UV treatment, *Environ. Int.* 35 (2009) 793–802, <https://doi.org/10.1016/j.envint.2009.01.003>.
- [17] R. Liang, A. Hu, W. Li, Y.N. Zhou, Enhanced degradation of persistent pharmaceuticals found in wastewater treatment effluents using TiO<sub>2</sub> nanobelt photocatalysts, *J. Nanoparticle Res.* 15 (2013) 1990, <https://doi.org/10.1007/s11051-013-1990-x>.
- [18] S. Sun, J. Jiang, S. Pang, J. Ma, M. Xue, J. Li, Y. Liu, Y. Yuan, Oxidation of theophylline by Ferrate (VI) and formation of disinfection byproducts during subsequent chlorination, *Sep. Purif. Technol.* 201 (2018) 283–290, <https://doi.org/10.1016/j.seppur.2018.03.014>.
- [19] A. Ghauch, A. Baalbaki, M. Amasha, R. El Asmar, O. Tantawi, R. El Asmar, O. Tantawi, Contribution of persulfate in UV-254 nm activated systems for complete degradation of chloramphenicol antibiotic in water, *Chem. Eng. J.* 317 (2017) 1012–1025, <https://doi.org/10.1016/j.cej.2017.02.133>.
- [20] M. Amasha, A. Baalbaki, S. Al Hakim, R. El Asmar, A. Ghauch, Degradation of a Toxic Molecule o-Toluidine in Industrial Effluents using UV254/PS System, *J. Adv. Oxid. Technol.* 21 (n.d.) 261–273. <https://www.ingentaconnect.com/content/sycamore/jaot/2018/00000021/00000001/art00023>.
- [21] M. Amasha, A. Baalbaki, A. Ghauch, A comparative study of the common persulfate activation techniques for the complete degradation of an NSAID: the case of ketoprofen, *Chem. Eng. J.* 350 (2018) 395–410, <https://doi.org/10.1016/j.cej.2018.05.118>.
- [22] G. Mark, M.N. Schuchmann, H.P. Schuchmann, C. von Sonntag, The photolysis of potassium peroxodisulphate in aqueous solution in the presence of tert-butanol: a simple actinometer for 254 nm radiation, *J. Photochem. Photobiol. A Chem.* (1990), [https://doi.org/10.1016/1010-6030\(90\)80028-V](https://doi.org/10.1016/1010-6030(90)80028-V).
- [23] Y. Gao, N. Gao, Y. Deng, Y. Yang, Y. Ma, Ultraviolet (UV) light-activated persulfate oxidation of sulfamethazine in water, *Chem. Eng. J.* 195 (2012) 248–253, <https://doi.org/10.1016/j.cej.2012.04.084>.
- [24] L. Bu, S. Zhou, S. Shi, L. Deng, G. Li, Q. Yi, N. Gao, Degradation of oxcabazepine by UV-activated persulfate oxidation: kinetics, mechanisms, and pathways, *Environ. Sci. Pollut. Res.* 23 (2016) 2848–2855, <https://doi.org/10.1007/s11356-015-5524-1>.
- [25] C. Tan, N. Gao, S. Zhou, Y. Xiao, Z. Zhuang, Kinetic study of acetaminophen degradation by UV-based advanced oxidation processes, *Chem. Eng. J.* (2014), <https://doi.org/10.1016/j.cej.2014.05.013>.
- [26] Abbas Baalbaki, Nagham Zein Eddine, Saly Jaber, Maya Amasha, Antoine Ghauch, Rapid quantification of persulfate in aqueous systems using a modified HPLC unit, *Talanta* 178 (2018) 237–245, <https://doi.org/10.1016/j.talanta.2017.09.036>.
- [27] X. Ao, W. Liu, Degradation of sulfamethoxazole by medium pressure UV and oxidants: peroxymonosulfate, persulfate, and hydrogen peroxide, *Chem. Eng. J.* 313 (2017) 629–637, <https://doi.org/10.1016/j.cej.2016.12.089>.
- [28] V.J. Pereira, K.G. Linden, H.S. Weinberg, Evaluation of UV irradiation for photolytic and oxidative degradation of pharmaceutical compounds in water, *Water Res.* 41 (2007) 4413–4423, <https://doi.org/10.1016/j.watres.2007.05.056>.
- [29] C. Qi, X. Liu, C. Lin, X. Zhang, J. Ma, H. Tan, W. Ye, Degradation of sulfamethoxazole by microwave-activated persulfate: Kinetics, mechanism and acute toxicity, *Chem. Eng. J.* 249 (2014) 6–14, <https://doi.org/10.1016/j.cej.2014.03.086>.
- [30] X. Lu, Y. Shao, N. Gao, J. Chen, Y. Zhang, H. Xiang, Y. Guo, Degradation of diclofenac by UV-activated persulfate process: Kinetic studies, degradation pathways and toxicity assessments, *Ecotoxicol. Environ. Saf.* 141 (2017) 139–147, <https://doi.org/10.1016/j.ecoenv.2017.03.022>.
- [31] S. Dhaka, R. Kumar, M.A. Khan, K.-J. Paeng, M.B. Kurade, S.-J. Kim, B.-H. Jeon, Aqueous phase degradation of methyl paraben using UV-activated persulfate method, *Chem. Eng. J.* 321 (2017) 11–19, <https://doi.org/10.1016/j.cej.2017.03.085>.
- [32] L.W. Matzek, K.E. Carter, Activated persulfate for organic chemical degradation: a review, *Chemosphere* 151 (2016) 178–188, <https://doi.org/10.1016/j.chemosphere.2016.02.055>.
- [33] A. Ghauch, G. Ayoub, S. Naim, Degradation of sulfamethoxazole by persulfate assisted micrometric Fe<sup>0</sup> in aqueous solution, *Chem. Eng. J.* (2013), <https://doi.org/10.1016/j.cej.2013.05.045>.
- [34] T. Olmez-Hanci, I. Arslan-Alaton, Comparison of sulfate and hydroxyl radical based advanced oxidation of phenol, *Chem. Eng. J.* 224 (2013) 10–16, <https://doi.org/10.1016/j.cej.2012.11.007>.
- [35] J. Rodríguez-Chueca, S. Giannakis, M. Marjanovic, M. Kohantorabi, M.R. Gholami, D. Grandjean, L.F. de Alencastro, C. Pulgarín, Solar-assisted bacterial disinfection and removal of contaminants of emerging concern by Fe<sup>2+</sup>-activated HSO<sup>-</sup> vs. S<sup>2-</sup> in drinking water, *Appl. Catal. B Environ.* (2019), <https://doi.org/10.1016/j.apcatb.2019.02.018>.
- [36] D.A. House, Kinetics and mechanism of oxidations by peroxydisulfate, *Chem. Rev.* (1962), <https://doi.org/10.1021/cr60217a001>.
- [37] A. Ghauch, A.M. Tuqan, N. Kibbi, Ibuprofen removal by heated persulfate in aqueous solution: a kinetics study, *Chem. Eng. J.* 197 (2012) 483–492, <https://doi.org/10.1016/j.cej.2012.05.051>.
- [38] C.-W. Wang, C. Liang, Oxidative degradation of TMAH solution with UV persulfate activation, *Chem. Eng. J.* 254 (2014) 472–478, <https://doi.org/10.1016/j.cej.2014.05.116>.
- [39] Dissociation constants of organic acids in aqueous solution, *Pure Appl. Chem.* 1 (1960) 187. <http://dx.doi.org/10.1351/pac196001020187>.
- [40] L. Chen, T. Cai, C. Cheng, Z. Xiong, D. Ding, Degradation of acetamiprid in UV/H<sub>2</sub>O<sub>2</sub> and UV/persulfate systems: a comparative study, *Chem. Eng. J.* 351 (2018) 1137–1146, <https://doi.org/10.1016/j.cej.2018.06.107>.
- [41] C. Liang, H.-W. Su, Identification of sulfate and hydroxyl radicals in thermally activated persulfate, *Ind. Eng. Chem. Res.* 48 (2009) 5558–5562, <https://doi.org/10.1021/ie9002848>.
- [42] H.A. Gorrell, Classification of formation waters based on sodium chloride content: geological notes, *Am. Assoc. Pet. Geol. Bull.* 42 (1958) 2513.
- [43] Environment Protection Authority (EPA) in South Australia, Salinity, Environ. Info. (n.d.). [http://www.epa.sa.gov.au/environmental\\_info/water\\_quality/threats/salinity](http://www.epa.sa.gov.au/environmental_info/water_quality/threats/salinity) (accessed June 15, 2017).
- [44] A. Angkaw, C. Sakulthaew, T. Satapanajaru, C. Chokejaroenrat, UV-activated persulfate oxidation of 17 $\beta$ -estradiol: Implications for discharge water remediation, *J. Environ. Chem. Eng.* (2018) 102858, <https://doi.org/10.1016/j.jece.2018.102858>.
- [45] Z. Fang, P. Chelme-Ayala, Q. Shi, C. Xu, M. Gamal El-Din, Degradation of naphthenic acid model compounds in aqueous solution by UV activated persulfate: influencing factors, kinetics and reaction mechanisms, *Chemosphere* (2018), <https://doi.org/10.1016/j.chemosphere.2018.07.132>.
- [46] X. Gu, S. Lu, L. Li, Z. Qiu, Q. Sui, K. Lin, Q. Luo, Oxidation of 1,1,1-trichloroethane stimulated by thermally activated persulfate, *Ind. Eng. Chem. Res.* 50 (2011) 11029–11036, <https://doi.org/10.1021/ie201059x>.
- [47] H. Gao, J. Chen, Y. Zhang, X. Zhou, Sulfate radicals induced degradation of Triclosan in thermally activated persulfate system, *Chem. Eng. J.* 306 (2016) 522–530, <https://doi.org/10.1016/j.cej.2016.07.080>.
- [48] L. Zhou, C. Ferronato, J.M. Chovelon, M. Sleiman, C. Richard, Investigations of diatrizoate degradation by photo-activated persulfate, *Chem. Eng. J.* (2017), <https://doi.org/10.1016/j.cej.2016.11.066>.
- [49] Y. Gao, N. Gao, Y. Deng, D. Yin, Y. Zhang, Degradation of florfenicol in water by UV/Na<sub>2</sub>S<sub>2</sub>O<sub>8</sub> process, *Environ. Sci. Pollut. Res.* 22 (2015) 8693–8701, <https://doi.org/10.1007/s11356-014-4054-6>.
- [50] Y. Fan, Y. Ji, D. Kong, J. Lu, Q. Zhou, Kinetic and mechanistic investigations of the degradation of sulfamethazine in heat-activated persulfate oxidation process, *J. Hazard. Mater.* (2015), <https://doi.org/10.1016/j.jhazmat.2015.06.058>.
- [51] S. Norzaee, M. Taghavi, B. Djahed, F.K. Mostafapour, Degradation of Penicillin G by heat activated persulfate in aqueous solution, *J. Environ. Manage.* 215 (2018) 316–323, <https://doi.org/10.1016/j.jenvman.2018.03.038>.
- [52] S. Wang, J. Wu, X. Lu, W. Xu, Q. Gong, J. Ding, B. Dan, P. Xie, Removal of acetaminophen in the Fe<sup>2+</sup>/persulfate system: Kinetic model and degradation pathways, *Chem. Eng. J.* 358 (2019) 1091–1100, <https://doi.org/10.1016/j.cej.2018.09.145>.
- [53] C. Tan, N. Gao, Y. Deng, W. Rong, S. Zhou, N. Lu, Degradation of antipyrine by heat activated persulfate, *Sep. Purif. Technol.* 109 (2013) 122–128, <https://doi.org/10.1016/J.SEPUR.2013.03.003>.
- [54] D. Miao, J. Peng, X. Zhou, L. Qian, M. Wang, L. Zhai, S. Gao, Oxidative degradation of atenolol by heat-activated persulfate: Kinetics, degradation pathways and distribution of transformation intermediates, *Chemosphere* 207 (2018) 174–182, <https://doi.org/10.1016/j.chemosphere.2018.05.068>.
- [55] A. Ghauch, A.M. Tuqan, Oxidation of bisoprolol in heated persulfate/H<sub>2</sub>O systems:

- kinetics and products, *Chem. Eng. J.* (2012), <https://doi.org/10.1016/j.cej.2011.12.048>.
- [56] C. Liang, Z.-S. Wang, N. Mohanty, Influences of carbonate and chloride ions on persulfate oxidation of trichloroethylene at 20 °C, *Sci. Total Environ.* 370 (2006) 271–277, <https://doi.org/10.1016/j.scitotenv.2006.08.028>.
- [57] K. Hasegawa, P. Neta, Rate constants and mechanisms of reaction of Cl<sub>2</sub>-radicals, *J. Phys. Chem.* 82 (1978) 854–857.
- [58] D.A. Armstrong, R.E. Huie, S. Lymar, W.H. Koppenol, G. Merényi, P. Neta, D.M. Stanbury, S. Steenken, P. Wardman, Standard electrode potentials involving radicals in aqueous solution: Inorganic radicals, *Bioinorg. React. Mech.* (2013), <https://doi.org/10.1515/irm-2013-0005>.
- [59] J. Kiwi, A. Lopez, V. Nadtochenko, Mechanism and kinetics of the OH-radical intervention during fenton oxidation in the presence of a significant amount of radical scavenger (Cl<sup>-</sup>), *Environ. Sci. Technol.* 34 (2000) 2162–2168, <https://doi.org/10.1021/es991406i>.
- [60] P.L. Brezonik, J. Fulkerson-Brekken, Nitrate-induced photolysis in natural waters: controls on concentrations of hydroxyl radical photo-intermediates by natural scavenging agents, *Environ. Sci. Technol.* 32 (1998) 3004–3010, <https://doi.org/10.1021/es9802908>.
- [61] D. Vione, S. Khanra, S.C. Man, P.R. Maddigapu, R. Das, C. Arsene, R.-I. Olariu, V. Maurino, C. Minero, Inhibition vs. enhancement of the nitrate-induced photo-transformation of organic substrates by the •OH scavengers bicarbonate and carbonate, *Water Res.* 43 (2009) 4718–4728, <https://doi.org/10.1016/j.watres.2009.07.032>.
- [62] G.-D. Fang, D.D. Dionysiou, S.R. Al-Abed, D.-M. Zhou, Superoxide radical driving the activation of persulfate by magnetite nanoparticles: Implications for the degradation of PCBs, *Appl. Catal. B Environ.* 129 (2013) 325–332, <https://doi.org/10.1016/j.apcatb.2012.09.042>.
- [63] Z.-H. Diao, J.-J. Liu, Y.-X. Hu, L.-J. Kong, D. Jiang, X.-R. Xu, Comparative study of Rhodamine B degradation by the systems pyrite/H<sub>2</sub>O<sub>2</sub> and pyrite/persulfate: reactivity, stability, products and mechanism, *Sep. Purif. Technol.* 184 (2017) 374–383, <https://doi.org/10.1016/j.seppur.2017.05.016>.
- [64] D.B. Miklos, C. Remy, M. Jekel, K.G. Linden, J.E. Drewes, U. Hübner, Evaluation of advanced oxidation processes for water and wastewater treatment – a critical review, *Water Res.* 139 (2018) 118–131, <https://doi.org/10.1016/j.watres.2018.03.042>.
- [65] E. Lipczynska-Kochany, G. Sprah, S. Harms, Influence of some groundwater and surface waters constituents on the degradation of 4-chlorophenol by the Fenton reaction, *Chemosphere* 30 (1995) 9–20, [https://doi.org/10.1016/0045-6535\(94\)00371-Z](https://doi.org/10.1016/0045-6535(94)00371-Z).
- [66] J.H. Baxendale, J.A. Wilson, The photolysis of hydrogen peroxide at high light intensities, *Trans. Faraday Soc.* (1957), <https://doi.org/10.1039/tf9575300344>.
- [67] Y. Yang, X. Lu, J. Jiang, J. Ma, G. Liu, Y. Cao, W. Liu, J. Li, S. Pang, X. Kong, C. Luo, Degradation of sulfamethoxazole by UV, UV/H<sub>2</sub>O<sub>2</sub> and UV/persulfate (PDS): formation of oxidation products and effect of bicarbonate, *Water Res.* (2017), <https://doi.org/10.1016/j.watres.2017.03.054>.
- [68] Z.X. Khoo, J.E.M. Teoh, Y. Liu, C.K. Chua, S. Yang, J. An, K.F. Leong, W.Y. Yeong, 3D printing of smart materials: a review on recent progresses in 4D printing, *Virtual Phys. Prototyp.* 10 (2015) 103–122, <https://doi.org/10.1080/17452759.2015.1097054>.
- [69] A. Darbi, T. Viraraghavan, Y.-C. Jin, L. Brul, D. Corkal, Sulfate removal from water, *Water Qual. Res. J.* 38 (2003) 169–182, <https://doi.org/10.2166/wqrj.2003.011>.
- [70] D.R. Hitchcock, Biogenic contributions to atmospheric sulphate levels, in: *Proc. Second Natl. Conf. Complet. Water Re-Use. Am. Inst. Chem. Eng. US Environ. Prot. Agency, Chicago, IL, May, 1975: p. 291*.
- [71] S.-Y. Oh, H.W. Kim, J.M. Park, H.S. Park, C. Yoon, Oxidation of polyvinyl alcohol by persulfate activated with heat, Fe<sup>2+</sup>, and zero-valent iron, *J. Hazard. Mater.* 168 (2009) 346–351, <https://doi.org/10.1016/j.jhazmat.2009.02.065>.
- [72] S.-Y. Oh, S.-G. Kang, P.C. Chiu, Degradation of 2, 4-dinitrotoluene by persulfate activated with zero-valent iron, *Sci. Total Environ.* 408 (2010) 3464–3468.
- [73] H. Zhang, Z. Wang, C. Liu, Y. Guo, N. Shan, C. Meng, L. Sun, Removal of COD from landfill leachate by an electro/Fe<sup>2+</sup>/peroxydisulfate process, *Chem. Eng. J.* 250 (2014) 76–82, <https://doi.org/10.1016/j.cej.2014.03.114>.
- [74] J. Yang, Z. Liu, Z. Zeng, Z. Huang, Y. Cui, A method for removing persulfate interference in the analysis of the chemical oxygen demand in wastewater, *Environ. Chem. Lett.* 17 (2019) 1085–1089, <https://doi.org/10.1007/s10311-018-00832-2>.
- [75] J.R. Bolton, K.G. Bircher, W. Tumas, C.A. Tolman, Figures-of-merit for the technical development and application of advanced oxidation technologies for both electric- and solar-driven systems (IUPAC Technical Report), *Pure Appl. Chem.* (2001), <https://doi.org/10.1351/pac200173040627>.
- [76] F. Fardoun, O. Ibrahim, R. Younes, H. Louahia-Gualous, Electricity of Lebanon: problems and recommendations, *Energy Procedia* 19 (2012) 310–320, <https://doi.org/10.1016/j.egypro.2012.05.211>.
- [77] XE Currency Converter: LBP to USD, (n.d.). <https://www.xe.com/currencyconverter/convert/?Amount=225&From=LBP&To=USD> (accessed December 16, 2018).